

EXPLORING THE DYNAMICS OF MONKEYPOX: A FRACTIONAL ORDER EPIDEMIC MODEL APPROACH

Isa Abdullahi Baba^{1,2}, Evren Hincal², Fathalla A. Rihan^{3,4}

¹ Department of Mathematics, Bayero University, Kano, Nigeria

² Department of Mathematics, Near East University, 99138 Mersin, Turkey

³ Department of Mathematical Sciences, College of Science, UAE University, Al Ain 15551, UAE

⁴ Department of Mathematics, Faculty of Science, Helwan University, Cairo 11795, Egypt
iababa.mth@buk.edu.ng, evren.hincal@neu.edu.tr, frihan@uaeu.ac.ae

Received: 15 September 2023; Accepted: 17 December 2023

Abstract. We present a mathematical model employing nonlinear fractional differential equations to investigate the transmission of disease from rodents to humans. The existence and uniqueness of the model's solutions are established through Banach contraction maps, and the local asymptotic stability of equilibrium solutions is confirmed. We calculate a critical parameter, the basic reproduction number, which reflects secondary infection rates. Numerical simulations illustrate dynamic changes over time, showcasing that our model provides a more comprehensive representation of the biological system compared to classical models.

MSC 2010: 92-08; 92B05

Keywords: fractional differential equations, disease transmission, rodents, Banach contraction mapping, basic reproduction number, numerical simulations

1. Introduction

Orthopoxviruses, primarily originating from wild rodents in Central and West Africa, are the main causative agents of Monkeypox, a zoonotic disease [1, 2]. It can spread through various mean, such as direct contact, sneezing, and saliva. The majority of infections result from contact with monkeys or rodents [3, 4]. Symptoms encompass fever, headache, body aches, followed by a blistering rash, swollen lymph nodes, and scarring [5, 6]. Severe cases are more prevalent in children and immunocompromised individuals, with complications affecting various organ systems [7]. In 2003, a Monkeypox epidemic was identified in the United States [8]. As of May 2022, the World Health Organization has reported 80 confirmed mild cases in 10 countries [8]. Mathematical models play a pivotal role in studying the dynamics of infectious diseases and offering guidance for epidemic control strategies. The limited focus on Monkeypox has impeded comprehensive understanding, although some researchers have developed deterministic models, providing insights

and proposing measures like quarantine [9–11]. Researchers in science and engineering are exploring fractional differential equations due to their memory effects, enhancing modeling techniques [12–15]. Fractional models applied to COVID-19 have demonstrated success [16–19], yet few studies have delved into Monkeypox transmission using fractional calculus [20, 21].

The objective of this paper was to analyse the transmission dynamics and control of Monkeypox in populations using a fractional-order model. The goal was to visualize how memory indices or fractional-order parameters influence the dynamics of Monkeypox disease and its impact on the dynamics of smallpox disease. Among the many models of Monkeypox in the literature, few have been constructed to explain the origin of the disease and its transmission in hospitals and care centers. In this paper, the origin of the virus is considered to be rodents, and it is incorporated into the model, taking various stages of infection into account.

The paper is organized as follows: Section 1 introduces the topic, Section 2 presents the model formulation, Section 3 discusses the existence and uniqueness of model solutions, and Section 4 covers the derivation of the basic reproduction number and the local stability analysis of the solution. Finally, Section 5 supports the analytical results with numerical simulations, presenting our discussion and conclusions.

2. Model formulation

With rodents as the origin of the monkeypox, it is assumed that the newborn rodents are born into susceptible class S_r , at the rate λ_r . Which joined the infectious class at rate β_1 . It is also assumed that the newborn of humans are born into susceptible class S_h which later became infectious I_h as a result of contact with an infected rodent at the rate β_2 . Then the virus spreads from an infected human to human H_h , to a family member F_m , then to clinic center P_c and care center C_c at the rates β_3 , β_4 , β_5 and β_6 respectively, μ_i , $i = 1, 2, \dots, 8$, natural death rates in S_r , I_r , S_h , I_h , H_h , F_m , P_c and C_c , compartments respectively, δ_i , $i = 1, 2, 3, \dots, 5$, disease induced death in I_r , S_h , I_h , H_h , F_m , P_c and C_c compartments respectively. Figure 1 gives the schematic diagram of the dynamics of the disease.

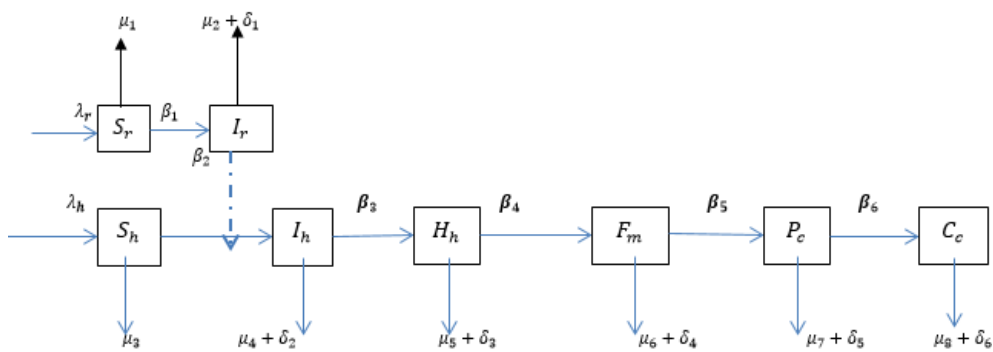


Fig. 1. Schematic diagram showing the dynamics of Monkeypox in a population

The transmission dynamics can be described by the nonlinear system of fractional order differential equations (FODE) in the sense of Caputo.

$${}^C_0D_t^\alpha S_r(t) = \lambda_r^\alpha - \mu_1^\alpha S_r - \beta_1^\alpha S_r I_r, \quad (1)$$

$${}^C_0D_t^\alpha I_r(t) = \beta_1^\alpha S_r I_r - (\mu_2^\alpha + \delta_1^\alpha) I_r - \beta_2^\alpha S_h I_r, \quad (2)$$

$${}^C_0D_t^\alpha S_h(t) = \lambda_h^\alpha - \mu_3^\alpha S_h - \beta_2^\alpha S_h I_r, \quad (3)$$

$${}^C_0D_t^\alpha I_h(t) = \beta_2^\alpha S_h I_r - (\mu_4^\alpha + \delta_2^\alpha) I_h - \beta_3^\alpha I_h H_h, \quad (4)$$

$${}^C_0D_t^\alpha H_h(t) = \beta_3^\alpha I_h H_h - (\mu_5^\alpha + \delta_3^\alpha) H_h - \beta_4^\alpha H_h F_m, \quad (5)$$

$${}^C_0D_t^\alpha F_m(t) = \beta_4^\alpha H_h F_m - (\mu_6^\alpha + \delta_4^\alpha) F_m - \beta_5^\alpha P_c F_m, \quad (6)$$

$${}^C_0D_t^\alpha P_c(t) = \beta_5^\alpha P_c F_m - (\mu_7^\alpha + \delta_5^\alpha) P_c - \beta_6^\alpha P_c C_c, \quad (7)$$

$${}^C_0D_t^\alpha C_c(t) = \beta_6^\alpha P_c C_c - (\mu_8^\alpha + \delta_6^\alpha) C_c, \quad (8)$$

where,

$$\begin{aligned} S_r(0) > 0, \quad I_r(0) \geq 0, \quad S_h(0) > 0, \quad I_h(0) \geq 0, \quad H_h(0) \geq 0, \quad F_m(0) \geq 0, \\ P_c(0) \geq 0, \quad C_c(0) \geq 0. \end{aligned}$$

3. Existence and uniqueness of the solutions

In this Section, we study the existence and uniqueness of solution of the model. Consider the following theorem,

Theorem 1. The kernels of equations (1)–(8) satisfy Lipschitz continuity for $L_i \geq 0, i = 1, 2, \dots, 8$.

PROOF: Let the kernels be

$$\begin{aligned} f_1(t, S_r) &= \lambda_r^\alpha - \mu_1^\alpha S_r - \beta_1^\alpha S_r I_r, \quad f_2(t, I_r) = \beta_1^\alpha S_r I_r - (\mu_2^\alpha + \delta_1^\alpha) I_r - \beta_2^\alpha S_h I_r, \\ f_3(t, S_h) &= \lambda_h^\alpha - \mu_3^\alpha S_h - \beta_2^\alpha S_h I_r, \quad f_4(t, I_h) = \beta_2^\alpha S_h I_r - (\mu_4^\alpha + \delta_2^\alpha) I_h - \beta_3^\alpha I_h H_h, \\ f_5(t, H_h) &= \beta_3^\alpha I_h H_h - (\mu_5^\alpha + \delta_3^\alpha) H_h - \beta_4^\alpha H_h F_m, \\ f_6(t, F_m) &= \beta_4^\alpha H_h F_m - (\mu_6^\alpha + \delta_4^\alpha) F_m - \beta_5^\alpha P_c F_m, \\ f_7(t, P_c) &= \beta_5^\alpha P_c F_m - (\mu_7^\alpha + \delta_5^\alpha) P_c - \beta_6^\alpha P_c C_c, \quad f_8(t, C_c) = \beta_6^\alpha P_c C_c - (\mu_8^\alpha + \delta_6^\alpha) C_c. \end{aligned}$$

Taking $f_1(t, S_r)$ and simplifying, we obtain

$$\|f_1(t, S_r) - f_1(t, S_r^*)\| \leq L_1 \|S_r - S_r^*\|. \quad (9)$$

In a similar way, we obtain

$$\begin{aligned}\|f_2(t, I_r) - f_2(t, I_r^*)\| &\leq L_2 \|I_r - I_r^*\|, \|f_3(t, S_h) - f_3(t, S_h^*)\| \leq L_3 \|S_h - S_h^*\|, \\ \|f_4(t, I_h) - f_4(t, I_h^*)\| &\leq L_4 \|I_h - I_h^*\|, \|f_5(t, H_h) - f_5(t, H_h^*)\| \leq L_5 \|H_h - H_h^*\|, \\ \|f_6(t, F_m) - f_6(t, F_m^*)\| &\leq L_6 \|F_m - F_m^*\|, \|f_7(t, P_c) - f_7(t, P_c^*)\| \leq L_7 \|P_c - P_c^*\|, \\ \|f_8(t, C_c) - f_8(t, C_c^*)\| &\leq L_8 \|C_c - C_c^*\|.\end{aligned}$$

To transform system (1) through (8) to equivalent Volterra-integral equations, we give the following Lemma:

Lemma 1: The continuous system (1) through (8) can be transformed to equivalent Volterra-integral equations.

Proof: Consider the integral of S_r that is,

$$S_r(t) = S_r(0) + \frac{1}{\Gamma(\alpha)} \int_0^t (t - \tau)^{\alpha-1} f_1(\tau, S_r(\tau)) dt. \quad (10)$$

Similarly,

$$\begin{aligned}I_r(t) &= I_r(0) + \frac{1}{\Gamma(\alpha)} \int_0^t (t - \tau)^{\alpha-1} f_2(\tau, I_r(\tau)) dt, \\ S_h(t) &= S_h(0) + \frac{1}{\Gamma(\alpha)} \int_0^t (t - \tau)^{\alpha-1} f_3(\tau, S_h(\tau)) dt, \\ I_h(t) &= I_h(0) + \frac{1}{\Gamma(\alpha)} \int_0^t (t - \tau)^{\alpha-1} f_4(\tau, I_h(\tau)) dt, \\ H_h(t) &= H_h(0) + \frac{1}{\Gamma(\alpha)} \int_0^t (t - \tau)^{\alpha-1} f_5(\tau, H_h(\tau)) dt, \\ F_m(t) &= F_m(0) + \frac{1}{\Gamma(\alpha)} \int_0^t (t - \tau)^{\alpha-1} f_6(\tau, F_m(\tau)) dt, \\ P_c(t) &= P_c(0) + \frac{1}{\Gamma(\alpha)} \int_0^t (t - \tau)^{\alpha-1} f_7(\tau, P_c(\tau)) dt, \\ C_c(t) &= C_c(0) + \frac{1}{\Gamma(\alpha)} \int_0^t (t - \tau)^{\alpha-1} f_8(\tau, C_c(\tau)) dt.\end{aligned}$$

Theorem 2. Let $0 < \alpha < 1$, $I = [0, h^*] \subseteq \mathbb{R}$ and $J = \{S_r(t) - S_r(0) \mid |S_r(t) - S_r(0)| \leq k_1\}$, let $f_1: I \times J \rightarrow \mathbb{R}$ be continuous bounded function, that is $\exists! M > 0$ such that $|f_i(t, S_r)| \leq M_1$. Assume that f_1 satisfy Lipschitz condition, if $L_1 k_1 < M_1$, then there exist unique $S_r \in C[0, h^*]$, $h^* = \min\left[h, \left(\frac{k_1 \Gamma(\alpha+1)}{M_1}\right)^{\frac{1}{\alpha}}\right]$.

PROOF: Let $T = \{S_r \in C[0, h^*] : \|S_r(t) - S_r(0)\| \leq k_1\}$, since $T \subseteq \mathbb{R}$ and its closed set, then T is a complete metric space. From (10), define operator F in T , such that

$$FS_r(t) = S_r(0) + \frac{1}{\Gamma(\alpha)} \int_0^t (t-\tau)^{\alpha-1} f_1(\tau, S_r(\tau)) d\tau. \quad (11)$$

Then,

$$|FS_r(t) - S_r(0)| \leq k_1. \quad (12)$$

Similarly,

$$\begin{aligned} |FI_r(t) - I_r(0)| &\leq k_2, \quad |FS_h(t) - S_h(0)| \leq k_3, \quad |FI_h(t) - I_h(0)| \leq k_4, \\ |FH_h(t) - H_h(0)| &\leq k_5, \\ |FF_m(t) - F_m(0)| &\leq k_6, \quad |FP_c(t) - P_c(0)| \leq k_7, \quad |FC_c(t) - C_c(0)| \leq k_8. \end{aligned}$$

Therefore F maps T onto itself. Secondly, to show that T is contractive, we have

$$FS_r - FS_r^* = S_r(0) - S_r^*(0) + \frac{1}{\Gamma(\alpha)} \int_0^t (t-\tau)^{\alpha-1} [f_1(\tau, S_r(\tau)) - f_1(\tau, S_r^*(\tau))] d\tau.$$

Since $S_r(0) = S_r^*(0)$, then

$$\begin{aligned} |FS_r - FS_r^*| &= \left| \frac{1}{\Gamma(\alpha)} \int_0^t (t-\tau)^{\alpha-1} [f_1(\tau, S_r(\tau)) - f_1(\tau, S_r^*(\tau))] d\tau \right| \\ &\leq \frac{1}{\Gamma(\alpha)} \int_0^t (t-\tau)^{\alpha-1} L_1 \|S_r - S_r^*\| d\tau \\ &= \frac{L_1}{\Gamma(\alpha+1)} \|S_r - S_r^*\| t^\alpha \leq \frac{L_1}{\Gamma(\alpha+1)} \|S_r - S_r^*\| \frac{k_1 \Gamma(\alpha+1)}{M_1}. \end{aligned}$$

Hence, we get

$$\|FS_r - FS_r^*\| \leq \frac{L_1 k_1}{M_1} \|S_r - S_r^*\|. \quad (13)$$

Since by hypothesis $\frac{L_1 k_1}{M_1} < 1$, then T is contractive and has a unique fixed point. In a similar way, we obtain

$$\begin{aligned} \|FI_r - FI_r^*\| &\leq \frac{L_2 k_2}{M_2} \|I_r - I_r^*\|, \quad \|FS_h - FS_h^*\| \leq \frac{L_3 k_3}{M_3} \|S_h - S_h^*\|, \\ \|FI_h - FI_h^*\| &\leq \frac{L_4 k_4}{M_4} \|I_h - I_h^*\|, \quad \|FH_h - FH_h^*\| \leq \frac{L_5 k_5}{M_5} \|H_h - H_h^*\|, \\ \|FF_m - FF_m^*\| &\leq \frac{L_6 k_6}{M_6} \|F_m - F_m^*\|, \quad \|FP_c - FP_c^*\| \leq \frac{L_7 k_7}{M_7} \|P_c - P_c^*\|, \\ \|FC_c - FC_c^*\| &\leq \frac{L_8 k_8}{M_8} \|C_c - C_c^*\|. \end{aligned}$$

4. Basic reproduction ratio and stability analysis

In this chapter, we find the equilibrium solutions, the basic reproduction ratio and carry out local stability analysis of the solutions.

4.1. Equilibriums solutions

Equating system (1) through (8) to zero and solving simultaneously, we find two equilibrium solutions; disease – free (E_0) and endemic (E_1).

Disease free equilibrium E_0 is obtained by equating I_r , I_h , H_h , F_m , P_c and C_c to zero. Hence we get,

$$E_0 = \left(\frac{\lambda_r^\alpha}{\mu_1^\alpha}, 0, \frac{\lambda_h^\alpha}{\mu_3^\alpha}, 0, 0, 0, 0, 0 \right).$$

The endemic equilibrium is obtained by taking all the variables to be different from zero. We get

$$P_c^* = \frac{(\mu_8^\alpha + \delta_6^\alpha)}{\beta_6^\alpha}, \quad H_h^* = \frac{1}{\beta_4^\alpha} \left[\mu_6^\alpha + \delta_4^\alpha + \frac{\beta_5^\alpha (\mu_8^\alpha + \delta_6^\alpha)}{\beta_6^\alpha} \right], \quad S_r^* = \frac{\lambda_r^\alpha}{\mu_1^\alpha + \beta_1^\alpha I_r^*},$$

$$S_h^* = \frac{\lambda_h^\alpha}{\mu_3^\alpha + \beta_2^\alpha I_r^*},$$

$$I_r^* = \frac{1}{2} \left[\frac{\lambda_r^\alpha - \lambda_h^\alpha}{\mu_2^\alpha + \delta_1^\alpha} + \frac{\mu_1^\alpha}{\beta_1^\alpha} + \frac{\mu_1^\alpha}{\beta_2^\alpha} \right. \\ \left. \pm \sqrt{\left(\frac{\lambda_r^\alpha - \lambda_h^\alpha}{\mu_2^\alpha + \delta_1^\alpha} + \frac{\mu_1^\alpha}{\beta_1^\alpha} + \frac{\mu_1^\alpha}{\beta_2^\alpha} \right)^2 + \frac{4\lambda_r^\alpha \mu_3^\alpha}{\beta_2^\alpha (\mu_2^\alpha + \delta_1^\alpha)} \left(1 - \frac{\mu_1^\alpha (\mu_2^\alpha + \delta_1^\alpha) + \beta_2^\alpha \lambda_h^\alpha}{\beta_1^\alpha \lambda_r^\alpha} \right)} \right],$$

$$I_h^* = \frac{\beta_2^\alpha \beta_3^\alpha \beta_6^\alpha \lambda_h^\alpha I_r^*}{[\beta_4^\alpha \beta_6^\alpha (\mu_4^\alpha + \delta_2^\alpha) + \beta_3^\alpha \beta_6^\alpha (\mu_6^\alpha + \delta_4^\alpha) + \beta_3^\alpha \beta_5^\alpha (\mu_8^\alpha + \delta_6^\alpha)] (\mu_3^\alpha + \beta_2^\alpha I_r^*)},$$

$$F_m^* = \frac{\beta_2^\alpha \beta_3^\alpha \beta_6^\alpha \lambda_h^\alpha I_r^*}{[\beta_4^\alpha \beta_6^\alpha (\mu_4^\alpha + \delta_2^\alpha) + \beta_3^\alpha \beta_6^\alpha (\mu_6^\alpha + \delta_4^\alpha) + \beta_3^\alpha \beta_5^\alpha (\mu_8^\alpha + \delta_6^\alpha)] (\mu_3^\alpha + \beta_2^\alpha I_r^*)} \\ - \frac{1}{\beta_4^\alpha} (\mu_5^\alpha + \delta_3^\alpha),$$

and,

$$C_c^* = \frac{\beta_2^\alpha \beta_3^\alpha \beta_5^\alpha \lambda_h^\alpha I_r^*}{[\beta_4^\alpha \beta_6^\alpha (\mu_4^\alpha + \delta_2^\alpha) + \beta_3^\alpha \beta_6^\alpha (\mu_6^\alpha + \delta_4^\alpha) + \beta_3^\alpha \beta_5^\alpha (\mu_8^\alpha + \delta_6^\alpha)] (\mu_3^\alpha + \beta_2^\alpha I_r^*)} \\ - \frac{\beta_5^\alpha}{\beta_4^\alpha \beta_6^\alpha} (\mu_5^\alpha + \delta_3^\alpha) - \frac{1}{\beta_6^\alpha} (\mu_7^\alpha + \delta_5^\alpha).$$

4.2. Basic reproduction number

We will compute the basic reproduction number (R_0) using the next generation matrix method. Using next generation matrix, the basic reproduction number is the spectral radius of the next generation matrix $FV^{-1}(E_0)$ [22]. That is

$$R_0 = \rho(FV^{-1}(E_0)).$$

Now, let F be the transmission matrix and V the transition matrix obtained from (1)–(8). Also, let $F(E_0)$ and $V(E_0)$ be the Jacobian matrix obtained at disease – free equilibrium (E_0) with respect to F and V respectively. Then the basic reproduction ratio, R_0 is obtained to be,

$$R_0 = \rho(FV^{-1}(E_0)) = \frac{\beta_1^\alpha \lambda_r^\alpha}{\mu_1^\alpha (\mu_2^\alpha + \delta_1^\alpha) + \beta_2^\alpha \lambda_h^\alpha}.$$

4.3. Local stability analysis of the equilibria

From equations (1) through (8), Jacobian matrix is constructed

$$\begin{bmatrix} A & \beta_1^\alpha S_r & 0 & 0 & 0 & 0 & 0 & 0 \\ \beta_1^\alpha I_r & B & -\beta_2^\alpha I_r & 0 & 0 & 0 & 0 & 0 \\ 0 & -\beta_2^\alpha S_h & J & 0 & 0 & 0 & 0 & 0 \\ 0 & \beta_2^\alpha S_h & \beta_2^\alpha I_r & C & -\beta_3^\alpha I_h & 0 & 0 & 0 \\ 0 & 0 & 0 & \beta_3^\alpha H_h & D & -\beta_4^\alpha H_h & 0 & 0 \\ 0 & 0 & 0 & 0 & \beta_4^\alpha F_m & E & -\beta_4^\alpha F_m & 0 \\ 0 & 0 & 0 & 0 & 0 & \beta_5^\alpha P_c & G & -\beta_6^\alpha C_c \\ 0 & 0 & 0 & 0 & 0 & 0 & 0 & K \end{bmatrix},$$

where

$$\begin{aligned} A &= -\mu_1^\alpha - \beta_1^\alpha I_r, \quad B = \beta_1^\alpha S_r - (\mu_2^\alpha + \delta_1^\alpha) - \beta_2^\alpha S_h, \quad C = -(\mu_4^\alpha + \delta_2^\alpha) - \beta_3^\alpha H_h, \\ D &= \beta_3^\alpha I_h - (\mu_5^\alpha + \delta_3^\alpha) - \beta_4^\alpha F_m, \quad E = \beta_4^\alpha H_h - (\mu_6^\alpha + \delta_4^\alpha) - \beta_5^\alpha P_c, \\ G &= \beta_5^\alpha F_m - (\mu_7^\alpha + \delta_5^\alpha) - \beta_6^\alpha C_c, \quad J = \beta_6^\alpha P_c - (\mu_8^\alpha + \delta_6^\alpha), \quad K = \mu_3^\alpha - \beta_2^\alpha I_r. \end{aligned}$$

Theorem 3. The disease free equilibrium E_0 is locally asymptotically stable if $R_0 < 1$.

PROOF: Consider the Jacobian matrix at disease free equilibrium (E_0), then the eigenvalues are:

$$\begin{aligned} K_1 &= -\mu_1^\alpha, \quad K_2 = \beta_1^\alpha \frac{\lambda_b^\alpha}{\mu_1^\alpha} - (\mu_2^\alpha + \delta_1^\alpha) - \beta_2^\alpha \frac{\lambda_h^\alpha}{\mu_3^\alpha}, \quad K_3 = -\mu_3^\alpha, \quad K_4 = -(\mu_4^\alpha + \delta_2^\alpha), \\ K_5 &= -(\mu_5^\alpha + \delta_3^\alpha), \quad K_6 = -(\mu_6^\alpha + \delta_4^\alpha), \quad K_7 = -(\mu_7^\alpha + \delta_5^\alpha), \quad \text{and} \quad K_8 = -(\mu_8^\alpha + \delta_6^\alpha). \end{aligned}$$

All the eigenvalues are negative if $K_2 = \beta_1^\alpha \frac{\lambda_b^\alpha}{\mu_1^\alpha} - (\mu_2^\alpha + \delta_1^\alpha) - \beta_2^\alpha \frac{\lambda_h^\alpha}{\mu_3^\alpha} < 0$.

This is equivalent to

$$\frac{\beta_1^\alpha \lambda_r^\alpha}{\mu_1^\alpha (\mu_2^\alpha + \delta_1^\alpha) + \beta_2^\alpha \lambda_h^\alpha} < 1.$$

Hence, E_0 is locally asymptotically stable if $R_0 < 1$.

Theorem 4. The endemic equilibrium $(S_r^*, I_r^*, S_h^*, I_h^*, H_h^*, F_m^*, P_c^*, C_c^*)$ is stable if $R_0 > 1$.

PROOF: Consider the Jacobian matrix at endemic equilibrium (E_1) , our eigenvalues are;

$$\begin{aligned} K_1 &= A, \quad K_2 = -\frac{1}{2} \left[\sqrt{4\beta_1^\alpha I_r^* \beta_2^\alpha S_h^* + B^2 - 2BJ + J^2 + (B + J)} \right], \\ K_3 &= \frac{1}{2} \left[-\sqrt{4\beta_1^\alpha I_r^* \beta_2^\alpha S_h^* + B^2 - 2BJ + J^2 + (B + J)} \right], \\ K_4 &= -\frac{1}{2} \left[\sqrt{C^2 - 2CD - 4\beta_3^\alpha I_h^* \beta_3^\alpha H_h^* + (\beta_4^\alpha H_h^*)^2 + (C + \beta_4^\alpha H_h^*)} \right], \\ K_5 &= \frac{1}{2} \left[-\sqrt{C^2 - 2CD - 4\beta_3^\alpha I_h^* \beta_3^\alpha H_h^* + (\beta_4^\alpha H_h^*)^2 + (C + \beta_4^\alpha H_h^*)} \right], \\ K_6 &= E, K_6 = G, \text{ and } K_8 = K. \end{aligned}$$

Clearly, all the eigenvalues are negative if $R_0 > 1$.

5. Numerical simulations

In this section, the performance of the proposed model is tested by using Caputo differential operator using a fractional predictor-corrector method called, Adams-Bashforth-Moulton technique. Python is employed for conducting simulations in this paper. Convergence analysis of the method, as well as its error analysis can be found in [22]. Improving the efficiency or accuracy of the scheme, or exploring extensions to other related models would be very important for research in this direction, see for example [9, 17].

Numerical simulations using the following parameter values are carried out: $\beta_1 = 1.23$, $\beta_2 = 0.1$, $\beta_3 = 0.006$, $\beta_4 = 1.009$, $\beta_5 = 0.004$, $\beta_6 = 0.09$, $\lambda_r = 1.5$, $\lambda_h = 1.25$, $\mu_1 = 1.7$, $\mu_2 = 0.134$, $\mu_3 = 0.5$, $\mu_4 = 0.1343$, $\mu_5 = 0.0025$, $\mu_6 = 0.0074$, $\mu_7 = 0.344$, $\mu_8 = 0.5410$, $\delta_1 = 0.0143$, $\delta_2 = 0.3002$, $\delta_3 = 0.0054$, $\delta_4 = 0.0019$, $\delta_5 = 0.064$, $\delta_6 = 0.4400$.

From the graphs, we can see the richness in dynamics of biological systems when modeled with FODEs over the models with traditional integer – order.

The behaviour of susceptible rodents and humans can be seen in the Figure 2a, b where the required simulations have been carried out for $T = 10$ days while varying the values of the fractional order parameter α . It is observed that the population decay abruptly for higher values of the fractional-order parameter.

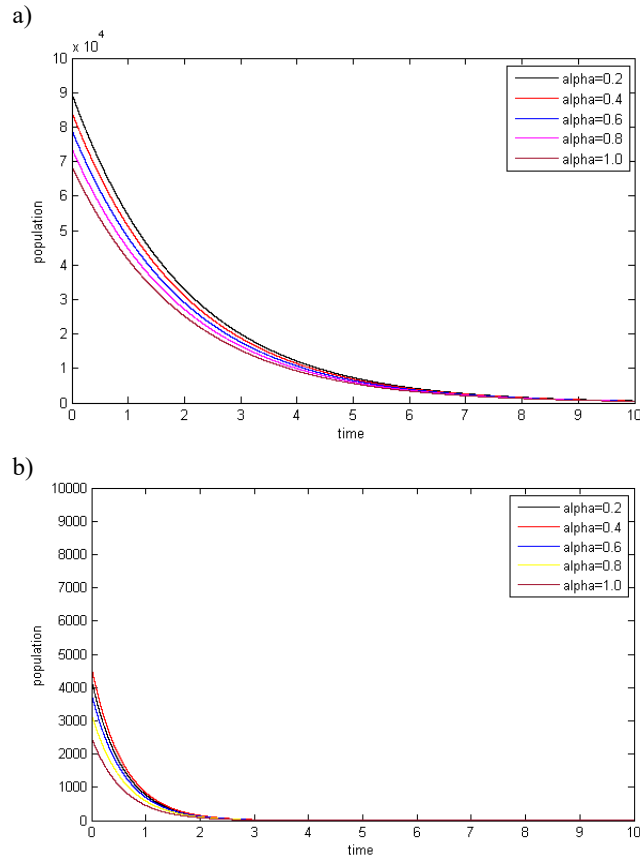


Fig. 2. Dynamics of susceptible rodents and humans respectively for varying fractional order α

In Figure 3a, both populations decline, with rodents declining more rapidly than humans due to the complexity of human behavior. Humans can receive treatment and employ survival strategies. In Figure 3b, both populations also decline, but susceptible rodents decline faster than susceptible humans because rodents lack preventive measures and infect each other rapidly, leading to widespread infection once they are exposed.

Figure 4 gives the dynamics of infected human, population of human that got infected through human, population of people that got infected through their family members, population of people that got infected from clinics, and population of people that got infected from care centers. Comparing the total infection I_h in the

population with that gotten directly from human infections, suggested that, larger portion of the infection is from the rodents.

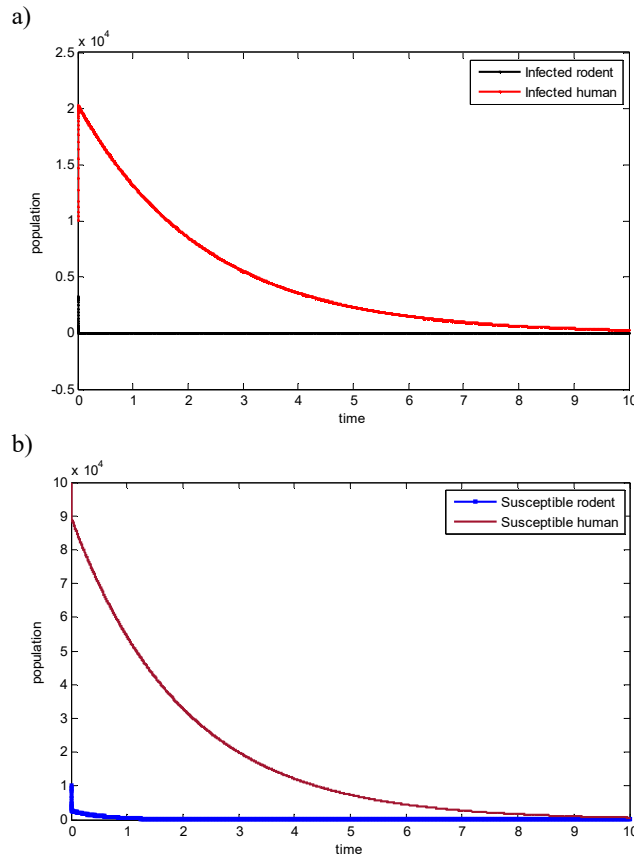


Fig. 3. Comparison of the dynamics of infected and susceptible rodents with infected and susceptible humans

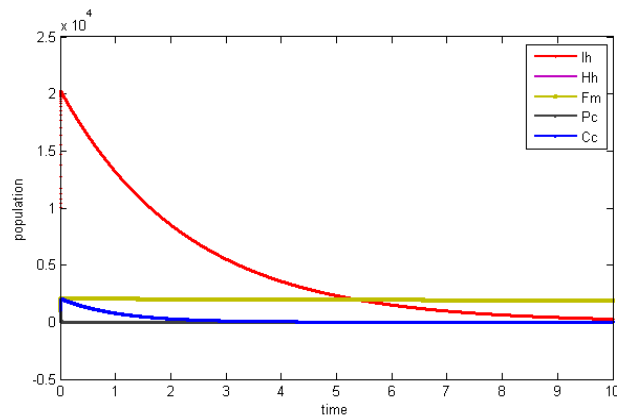


Fig. 4. Dynamics of all the infected classes in the human population

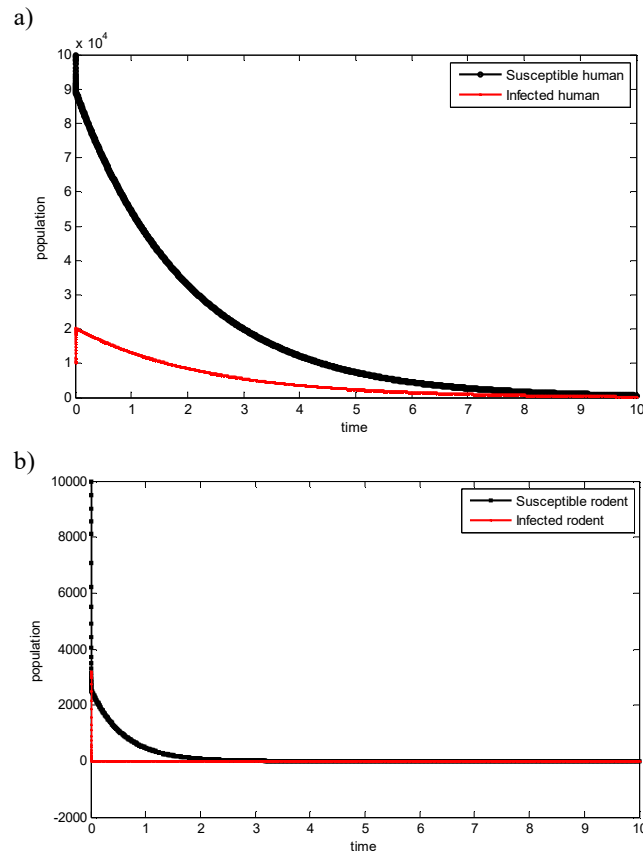


Fig. 5. Comparison of the dynamics of susceptible humans with infected humans

In Figure 5a, a comparison of susceptible and infected human dynamics reveals that both populations peak and decline almost simultaneously, influenced by factors such as natural death, disease-related mortality, and recovery. In Figure 5b, a similar comparison between susceptible and infected rodents shows that both populations also reach their peaks and decline nearly simultaneously, driven by factors such as natural death, disease-induced mortality, and natural recovery.

6. Conclusions

In conclusion, the utilization of fractional-order differential equations was observed to mitigate errors stemming from neglected parameters when modeling biological systems with memory and distributed system parameters. This paper introduced a Caputo-based fractional-order differential model for studying Monkeypox. The existence and uniqueness of the solution were established using the Banach contraction mapping principle. Local asymptotic stability was confirmed for equilibrium

solutions (disease-free and endemic), and the essential parameter, the basic reproduction number, was derived. Numerical simulations illustrated the dynamic changes over time in response to parameter variations. The numerical scheme used can be applied to other types of fractional derivatives.

The graphs also revealed that a significant portion of infections in the population originates from rodents rather than direct human-to-human transmission. Therefore, utmost caution must be exercised to prevent human contact with infected rodents. Future research could explore the integration of real-world data and environmental factors into the fractional differential model to improve the accuracy of disease transmission predictions.

References

- [1] Singh, N.P., Sharma, S., Ghai, G., & Singh, A. (2021). A systematic review on epidemiology of human Monkeypox virus. *Annals of the Romanian Society for Cell Biology*, 25(7), 602-610.
- [2] Sklenovská, N., & Van Ranst, M. (2018). Emergence of Monkeypox as the most important orthopoxvirus infection in humans. *Frontiers in Public Health*, 6, 241.
- [3] Oladoye, M.J. (2021). Monkeypox: a neglected viral zoonotic disease. *Electronic Journal of Medical and Educational Technologies*, 14(2), em2108.
- [4] Shanta, I.S., Luby, S.P., Hossain, K., Heffelfinger, J.D., Kilpatrick, A.M., Haider, N., ... & Gurley, E.S. (2023). Human exposure to bats, rodents and monkeys in Bangladesh. *EcoHealth*, 20(1), 53-64.
- [5] Deresinski, S. (2022). A case of Monkeypox in a returned traveler. *Infectious Disease Alert*, 41(8).
- [6] Jiang, R.M., Zheng, Y.J., Zhou, L., Feng, L.Z., Ma, L., Xu, B.P., ... & Shen, K.L. (2023). Diagnosis, treatment, and prevention of Monkeypox in children: an experts' consensus statement. *World Journal of Pediatrics*, 19(3), 231-242.
- [7] Costello, V., Sowash, M., Gaur, A., Cardis, M., Pasiaka, H., Wortmann, G., & Ramdeen, S. (2022). Imported Monkeypox from international traveler, Maryland, USA, 2021. *Emerging Infectious Diseases*, 28(5), 1002.
- [8] Peter, O.J., Kumar, S., Kumari, N., Oguntolu, F.A., Oshinubi, K., & Musa, R. (2022). Transmission dynamics of Monkeypox virus: a mathematical modelling approach. *Modeling Earth Systems and Environment*, 1-12.
- [9] Peter, O.J., Qureshi, S., Ojo, M.M., Viriyapong, R., & Soomro, A. (2023). Mathematical dynamics of measles transmission with real data from Pakistan. *Modeling Earth Systems and Environment*, 9(2), 1545-1558.
- [10] Baba, I.A., Nasidi, B.A., & Baleanu, D. (2021). Optimal control model for the transmission of novel COVID-19.
- [11] Baba, I.A., Yusuf, A., Nisar, K.S., Abdel-Aty, A.H., & Nofal, T.A. (2021). Mathematical model to assess the imposition of lockdown during COVID-19 pandemic. *Results in Physics*, 20, 103716.
- [12] Djennadi, S., Shawagfeh, N., Osman, M.S., Gómez-Aguilar, J.F., & Arqub, O.A. (2021). The Tikhonov regularization method for the inverse source problem of time fractional heat equation in the view of ABC-fractional technique. *Physica Scripta*, 96(9), 094006.
- [13] Ali, K.K., Abd El Salam, M.A., Mohamed, E.M., Samet, B., Kumar, S., & Osman, M.S. (2020). Numerical solution for generalized nonlinear fractional integro-differential equations with linear functional arguments using Chebyshev series. *Advances in Difference Equations*, 2020(1), 1-23.
- [14] Rashid, S., Kubra, K.T., Sultana, S., Agarwal, P., & Osman, M.S. (2022). An approximate analytical view of physical and biological models in the setting of Caputo operator via Elzaki

- transform decomposition method. *Journal of Computational and Applied Mathematics*, 413, 114378.
- [15] Yusuf, A., Qureshi, S., Mustapha, U.T., Musa, S.S., & Sulaiman, T.A. (2022). Fractional modeling for improving scholastic performance of students with optimal control. *International Journal of Applied and Computational Mathematics*, 8(1), 37.
- [16] Peter, O.J., Yusuf, A., Oshinubi, K., Oguntolu, F.A., Lawal, J.O., Abioye, A.I., & Ayoola, T.A. (2021). Fractional order of pneumococcal pneumonia infection model with Caputo Fabrizio operator. *Results in Physics*, 29, 104581.
- [17] Qureshi, S., & Jan, R. (2021). Modeling of measles epidemic with optimized fractional order under Caputo differential operator. *Chaos, Solitons & Fractals*, 145, 110766.
- [18] Peter, O.J. (2020). Transmission dynamics of fractional order Brucellosis model using Caputo-Fabrizio operator. *International Journal of Differential Equations*, 2020, 1-11.
- [19] Du, M., Wang, Z., & Hu, H. (2013). Measuring memory with the order of fractional derivative. *Scientific Reports*, 3(1), 3431.
- [20] El-Mesady, A., Elsonbaty, A., & Adel, W. (2022). On nonlinear dynamics of a fractional order Monkeypox virus model. *Chaos, Solitons & Fractals*, 164, 112716.
- [21] Majee, S., Jana, S., Barman, S., & Kar, T.K. (2023). Transmission dynamics of monkeypox virus with treatment and vaccination controls: A fractional order mathematical approach. *Physica Scripta*, 98(2), 024002.
- [22] Diethelm, K., Ford, N.J., & Freed, A.D. (2004). Detailed error analysis for a fractional Adams method. *Numerical Algorithms*, 36, 31-52.